Contents

2. Transient Response Measurements on a Satellite System

J.E. Nanevicz and R.C. Adamo
Electromagnetic Sciences Laboratory
Stanford Research Institute

1. BACKGROUND

In 1974, a set of instruments designed to detect the occurrence of electrical breakdowns was flown on a synchronous-orbit satellite. [1] The measurements make an interesting complement to those reported earlier at this conference by Bob Lovell of NASA LeRC. The LeRC sensors were installed on cables inside the vehicle. [2] Accordingly, they respond to signals coupled into the satellite wiring system. The SRI sensors were located on the exterior of the vehicle and detected the rf noise pulses associated with surface breakdowns.

The results of the earlier SRI program are being used to design and develop a set of instrumentation suitable for inclusion as a general piggy-back package for the detection of the onset of satellite charging and breakdowns on synchronous orbit satellites. This system will be flown as the Transient Pulse Monitor (TPM) system on the SCATHA spacecraft.

2. TEST SATELLITE INSTRUMENTATION

The instrumentation flown on the test satellite was capable of detecting the onset of geomagnetically disturbed conditions and of detecting and counting electrical breakdowns. [1] The system, shown in Figure 1, used a sensor plate mounted on the outside surface of the vehicle as both an electric dipole antenna to pick up noise pulses and as a Langmuir ion probe. Since the probe electrode was biased -5.6 volts with respect to the vehicle frame, it normally collected positive ions and repelled photoelectrons. Under disturbed conditions the ion probe system measures the differenc between the photoelectron current from the surface of the detector plate and the plasma electron current incident on the plate. Thus, substorms are indicated by a depressed probe current. Since the dc amplifier used with the ion probe system was unipolar, times when the current is reversed are indicated by a zero ion probe current reading.

Noise pulses induced in the sensor plate antenna are coupled through capacitor C to the preamplifier-counter electronics. Sensitivity tests of the pulse counting system were conducted using the set up shown in Figure 2. A thermal-control panel was placed inside a glass bell jar and illuminated with an electron beam to generate discharges from the mirror cells comprising the surface of the panel. The sensor electrode and electronics system flown on the flight vehicle were used to detect the noise pulses generated. Provisions were made to place the sensor at various distances from the edge of the thermal control. The results of these tests indicated that the pulse counter would reliably detect breakdowns within roughly a meter of the sensor plate.
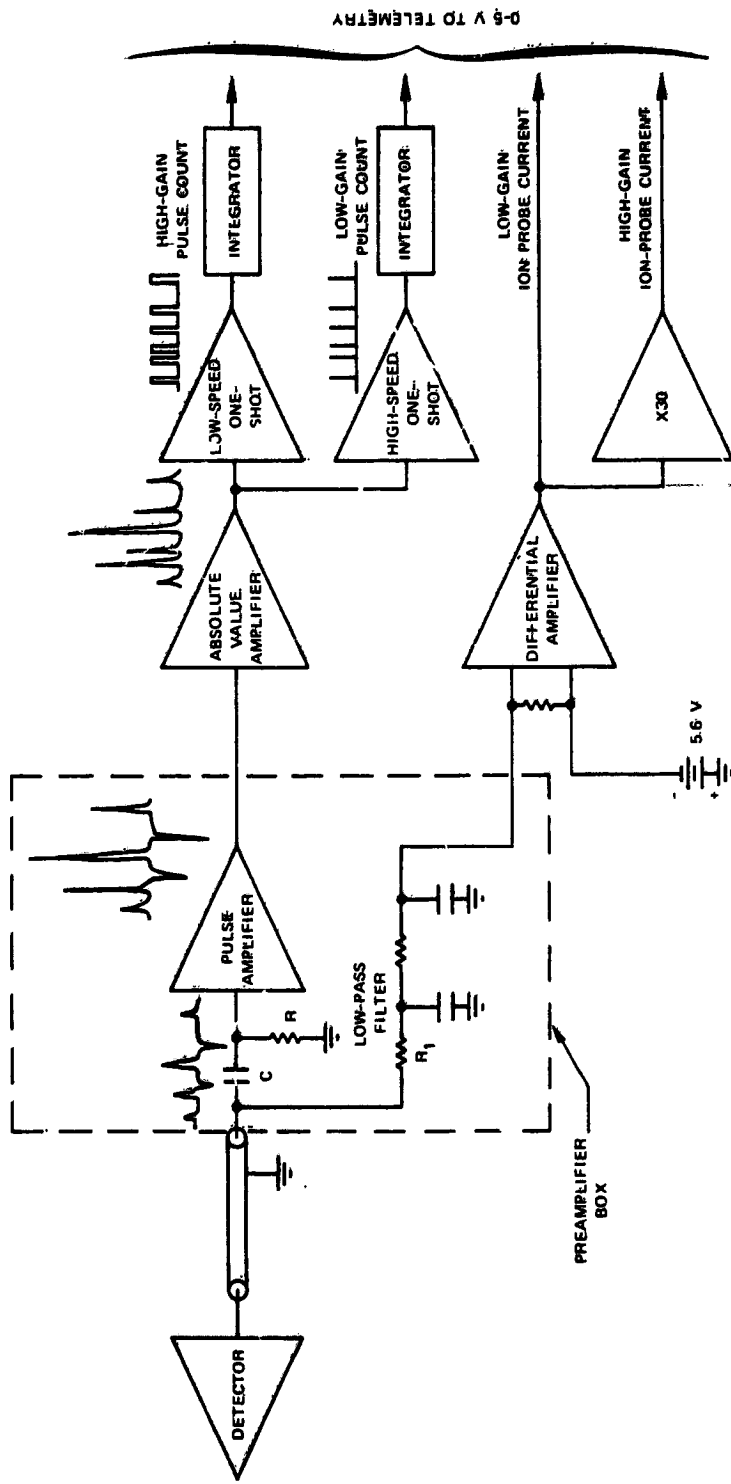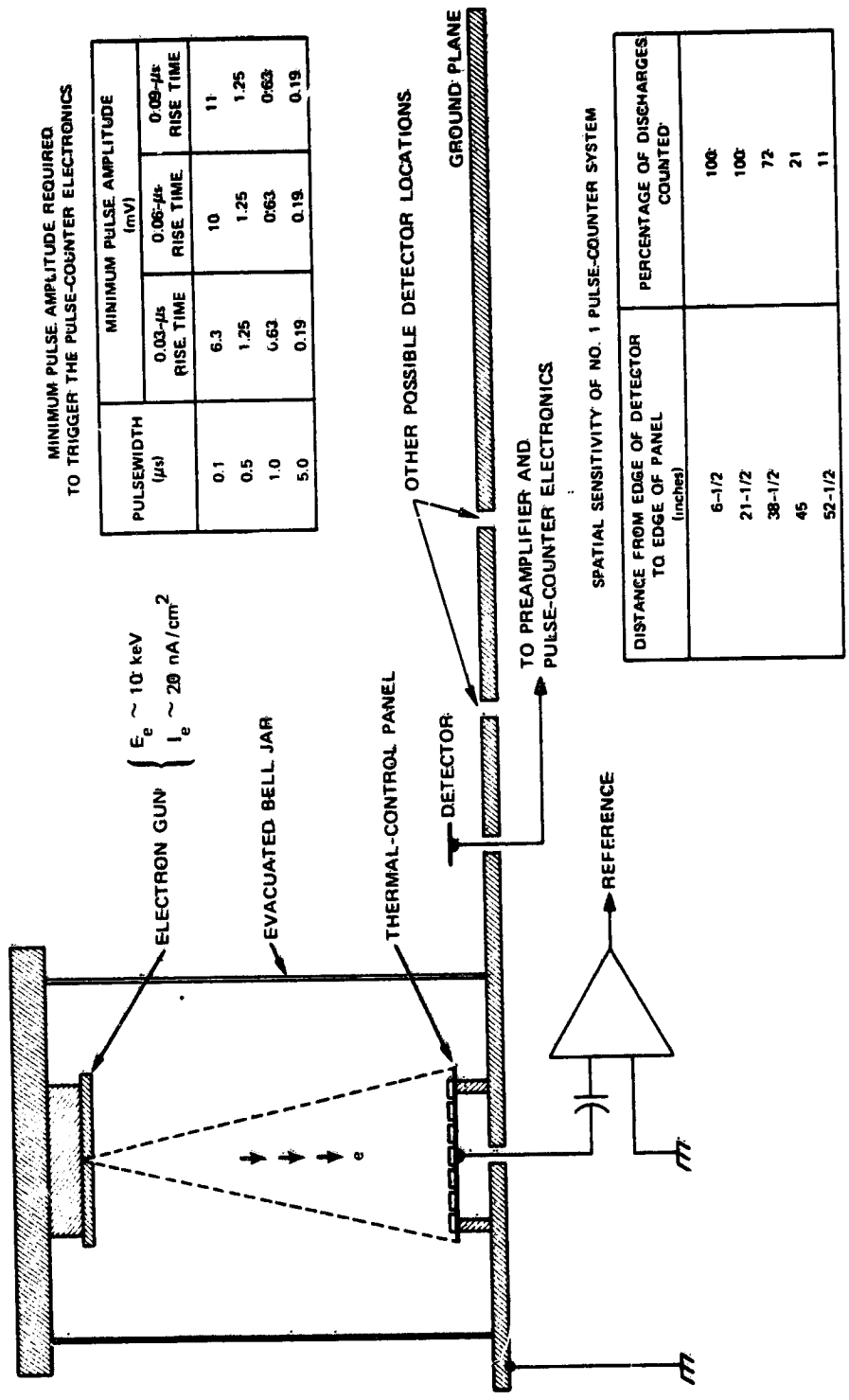
Figure 1. Block Diagram of Ion-Probe/Pulse-Counter System

MINIMUM PULSE AMPLITUDE REQUIRED
TO TRIGGER THE PULSE-COUNTER ELECTRONICS

PULSEWIDTH (μs)	MINIMUM PULSE AMPLITUDE (mV)		
	0.03-μs RISE TIME	0.06-μs RISE TIME	0.09-μs RISE TIME
0.1	6.3	10	11
0.5	1.25	1.25	1.25
1.0	0.63	0.63	0.63
5.0	0.19	0.19	0.19

SPATIAL SENSITIVITY OF NO. 1 PULSE-COUNTER SYSTEM

DISTANCE FROM EDGE OF DETECTOR TO EDGE OF PANEL (inches)	PERCENTAGE OF DISCHARGES COUNTED
6-1/2	100
21-1/2	100
38-1/2	72
45	21
52-1/2	11

ELECTRON GUN $\{\ E_e \sim 10\ keV,\ I_e \sim 20\ nA/cm^2 \}$

EVACUATED BELL JAR

THERMAL-CONTROL PANEL

DETECTOR

OTHER POSSIBLE DETECTOR LOCATIONS

GROUND PLANE

TO PREAMPLIFIER AND PULSE-COUNTER ELECTRONICS

REFERENCE

e

SA-2511-24R

Figure 2. Experimental Setup for Pulse-Counter Sensitivity Test

3. ORBITAL DATA

Figures 3 and 4 show data recorded during both undisturbed and disturbed geomagnetic field conditions for one complete satellite orbit. At synchronous altitudes, each orbit is 24 hr long, sampling all local times equally. Data from the ion-current probe are plotted as a function of local time (LT) in the upper panel of Figures 3 and 4. These data were selected at points in the satellite rotation at which the total probe current was a maximum (this corresponds to the orientation at which the detector plate is most nearly perpendicular to the sun direction resulting the maximum photoemission current). The geomagnetic field conditions were determined by examination of A_p and K_p shown at the top of Figures 3 and 4. Figure 3 shows data typically recorded during undisturbed geomagnetic field conditions. It shows the diurnal variation occurs because of the dependence of photoelectron current on the angle between the sun direction and the detector plate. At local evening and local morning the sun is normally incident to the detector plate, and the peak photoelectron current-density has a maximum of about 80 μA/m^2. At local midnight the sun is obliquely incident to the detector plate, and the peak photoelectric current has a minimum of about 30 μA/m^2. Near local noon the body of the spacecraft shadows the detector, and the photoelectron current is reduced nearly to zero, as shown from 10.7 – 13.3 hours LT in Figure 3. These data represent the usual diurnal variation of peak photoelectron current, and no depressions of the probe current indicating the injection of energetic electrons are observed.

The pulse-counter data are shown in the lower panels of Figures 3 and 4. The data plotted are the number of discharges per minute that are detected by the pulse counter. The number of counts were collected and averaged over a 10-min period. For the quiet geomagnetic period shown in Figure 3, few discharges are detected by the instrument except from local evening to local midnight during which rates averaging slightly less than 1/min are observed. Count rates typically near 30/hr are observed on almost every orbit from local evening to local midnight.

Figure 4 illustrates data recorded during an orbit on 31 January 1974 for which a moderate geomagnetic field disturbance was indicated by the magnetic indices. The injection of energetic electrons at synchronous altitude was detected by depressions of the total probe current caused by increases in the plasma-electron current during the injection event.

Two examples of data recorded during satellite eclipse are shown in Figures 5 and 6. Figure 5 shows the ion-current probe and pulse counter data recorded during undisturbed geomagnetic conditions. During satellite eclipse the probe current from the detector plate drops to nearly zero because solar ultraviolet radiation is not present to cause photoemission from the detector plate.
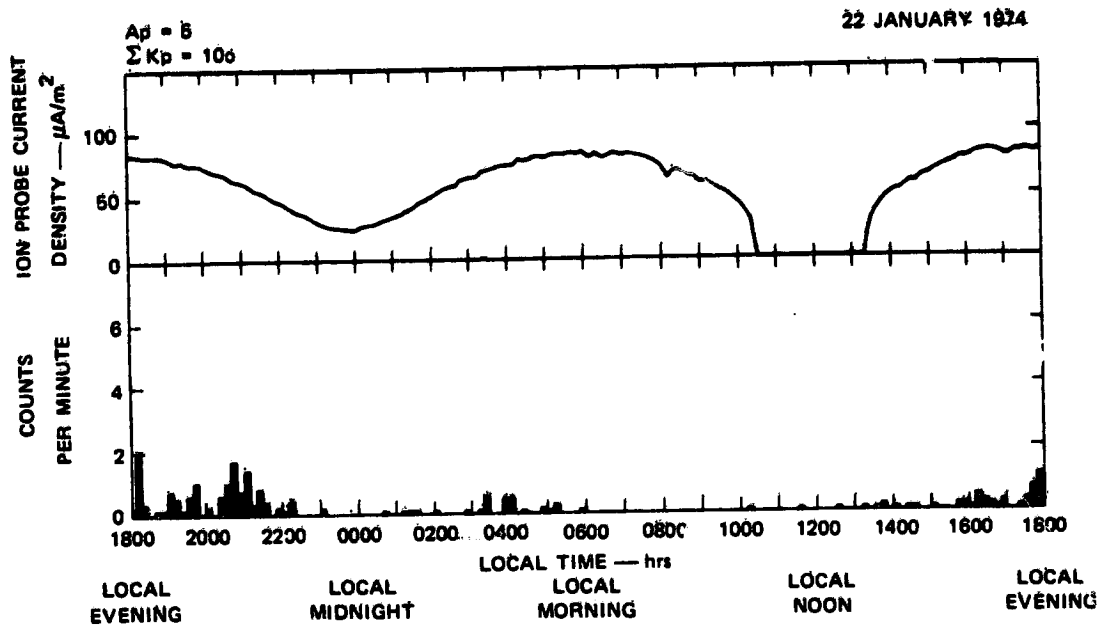
727

Figure 3. Static-Charge Experiment Data From an Orbit for which No Substorm Activity was Observed. (The ion-current probe data shows the usual diurnal variation. Few electrical discharges are observed except on the interval from local evening to local midnight.)
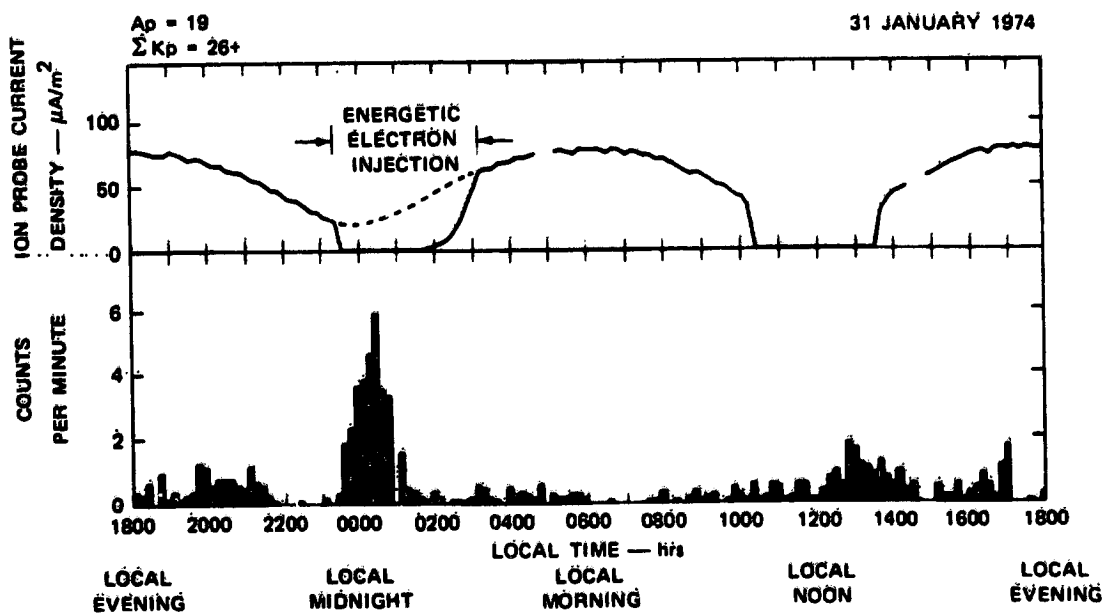

Figure 4. Static-Charge Experiment Data From an Orbit for which Substorm Activity was Observed. (Depressions of the ion-probe current near local midnight are caused by the injection of energetic electrons to synchronous altitudes. Discharge rates as high as six per minute are measured by the pulse counter during the electron injection event.)
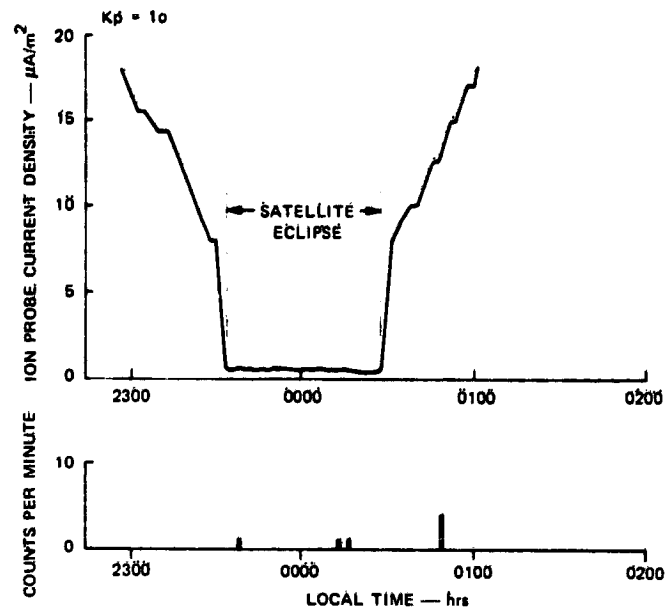
Figure 5. Static-Charge Experiment Data Recorded During Undisturbed Geomagnetic Field Conditions Through Satellite Eclipse. (The probe current drops to nearly zero when the photoelectric current is cut off by the earth's shadow. Only a few discharges are observed during this pass.)
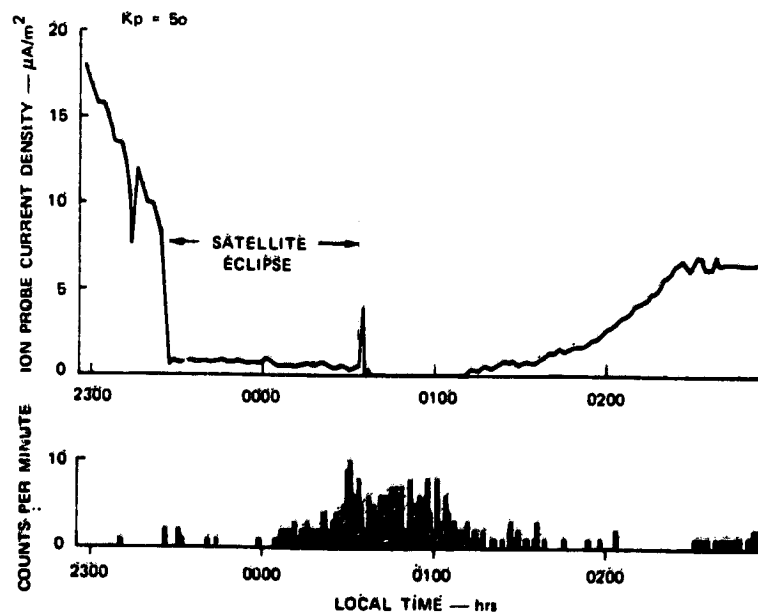

Figure 6. Static-Charge Experiment Data Recorded During Disturbed Geomagnetic Field Conditions Through Satellite Eclipse. (An energetic electron injection event and discharge rates as high as ten per minute are observed during this pass. The discharges are associated with the injection event (note depressed ion probe current) rather than with satellite eclipse.)

729

Smooth changes in the total probe current on either side of satellite eclipse are caused by changes in the satellite orientation (see Figure 3 and the related discussion of the diurnal variation in total probe current). Only a few pulse counts are observed by the pulse counter during this pass. (The pulse counter data are accumulated and averaged over a 2 min period for the data shown in Figures 5 and 6.)

Figure 6 shows an example of data recorded during a magnetospheric substorm near satellite eclipse. A depression of the ion probe current indicating the injection of energetic electrons is observed just after the satellite emerges from eclipse (compare these data with those shown in Figure 5). Discharge rates as high as 10/min are observed in association with this substorm electron-injection event.

The data in Figure 6 show that the discharges are associated with the injection of the energetic electrons near local midnight, and not with satellite eclipse. The beginning of the plasma-injection event shown in Figure 6 cannot be determined from the ion-current probe data because the satellite is in eclipse. It is possible that the discharge rates may have been enhanced during satellite eclipse; however the generating mechanism of the discharge is clearly the energetic plasma injection during the magnetospheric substorm.

These four examples of discharges observed by the static charge experiment are typical of the several conditions under which synchronous orbiting satellites must function. They show that electrical discharges are observed during substorms at rates near 10/min on the satellite's external surface. These discharges occur when energetic electrons are injected to synchronous altitudes near local midnight. These discharges are probably caused by the charging of dielectric surfaces to large negative potentials during the electron injection events.

Other discharges are observed near local evening and at other points in orbit at which discharges were not expected to occur. These discharges have lower rates (1/2 min); however, they occur on essentially all satellite orbits from local evening to local midnight. The generation of these discharges is not well understood at the time of this writing.

Several types of engineering orbital anomalies have occurred on this satellite that have been supposed to be related to electrical discharges. These anomalies consist of a type of anomalous detector response and an uncommanded reset of a satellite command circuit. These anomalies have occurred on several other satellites in addition to the satellite on which this experiment was flown. An examination of the values of ground-based geomagnetic indices at the times of occurrence of the anomalies strongly suggests that they are related to intense substorm activity. Thus, it was suggested that such anomalies were generated by interference from the electromagnetic radiation of electrical discharges.

During the period of operation of this experiment, several occurrences of both types of these anomalies were reported. For the anomalous detector response, a total of 35 occurrences were reported. For 31 of these cases a discharge was observed by the experiment coincidently with the anomalous detector response. These anomalous responses were reported on several different days, and the probability that the coincidences occurred by chance is essentially zero. There were a total of 6 of the uncommanded circuit resets, and 5 of these resets occurred coincidently with detection of discharges by the experiment. Thus, data from this experiment has confirmed the hypothesis that these types of orbital engineering anomalies are caused by interference from these electrical discharges.

4. SCATHA TRANSIENT PULSE MONITOR

Based on the experience gained in the satellite tests, a low-level program of planning and instrument development was initiated at SRI. The objective was the development of a set of compact, lightweight instruments to detect the occurrence of an electron injection event, to measure electric field E and current density J at the vehicle surface, and to detect, count, and characterize the pulse waveforms from electrical breakdowns on the satellite surface. A design goal was to develop simple instruments suitable for use on a piggy-back basis on a large number of satellites.

The pulse detection and characterization system will be repackaged and flown on the SCATHA satellite as a TPM. Although the TPM system can be used to measure pulses either on the outside or inside of the satellite, the SCATHA TPM system will be used entirely with internal sensors since the electromagnetic signature of the breakdown pulse on the exterior of the vehicle will be characterized by the SC1-2 experiment.

The purpose of the TPM system will be to acquire amplitude and pulse characteristics of transients coupled into vehicle power and signal lines when the spacecraft experiences arc discharges. Requirements imposed on the TPM system are as follows:

    (1) Measure peak pulse amplitude both + and - separately.

    (2) Determine number of transients absolute (+ and -).

    (3) Measure total energy both + and - separately.

    (4) Accomplish these measurements within the following constraints:

        (a) 60 dB dynamic range on amplifiers.

        (b) Select either a single pulse and/or multiple pulses.

        (c) Frequency response > 50 MHz.

These measurement capabilities are illustrated graphically in Figure 7.

SINGLE PULSE

THRESHOLD

+ PEAK AMPLITUDE
- PEAK AMPLITUDE
+ Σ ENERGY
- Σ ENERGY
ABSOLUTE NUMBER OF PULSES ABOVE THRESHOLD

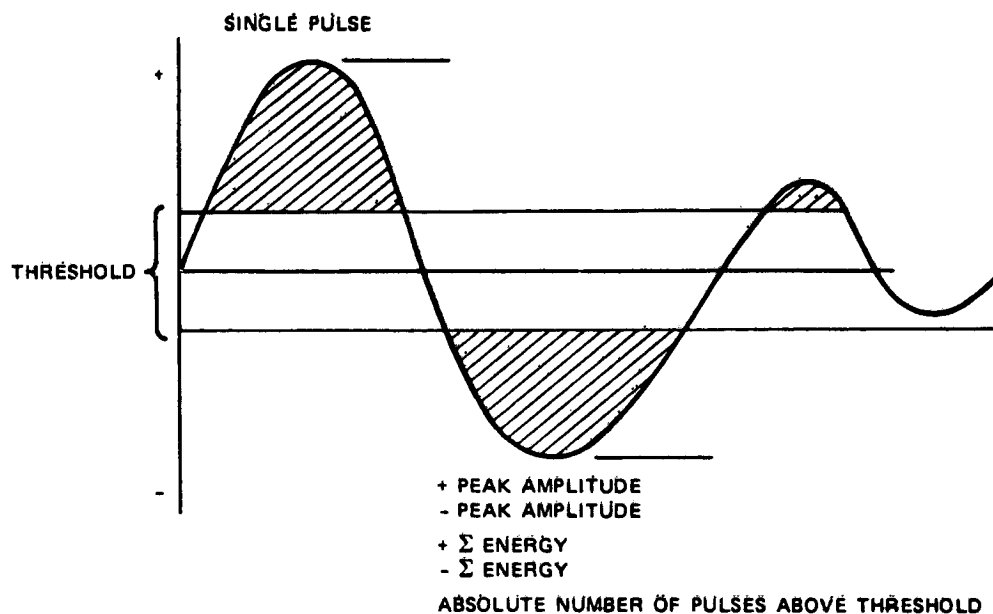Figure 7.   Data Derived From Transient-Pulse Monitor

The functional deployment of the TPM system will be as follows:

(1) Four (4) separate channels capable of yielding the complete data stipulated under requirements for each channel.

(2) Locations within the spacecraft will be:

      (a) Cable bundle antenna (low impedance).

      (b) Cable bundle antenna (high impedance).

      (c) Current probe on primary power reference ground.

      (d) Current probe on solar array power input.

A functional block diagram of the TPM is shown in Figure 8.   The ultimate form of the system stemmed from the requirement that it be able to provide information about the induced noise pulses even though the parameters of interest might vary over a considerable range.   Wide dynamic ranges were achieved in several ways.   First, logarithmic amplifier/detectors were used in the pulse-peak measuring system.   The pulse-integral measuring system has provisions for adjusting threshold in orbit to avoid the possibility of data being inadvertently contaminated by system noise.   Since it is not clear what the prf of breakdowns on SCATHA will be, provisions are included to command the pulse-peak and pulse-integral measuring systems to operate with a 1 sec measuring window or to operate for only 100 μsec after the first pulse occuring in a telemetry window.

732
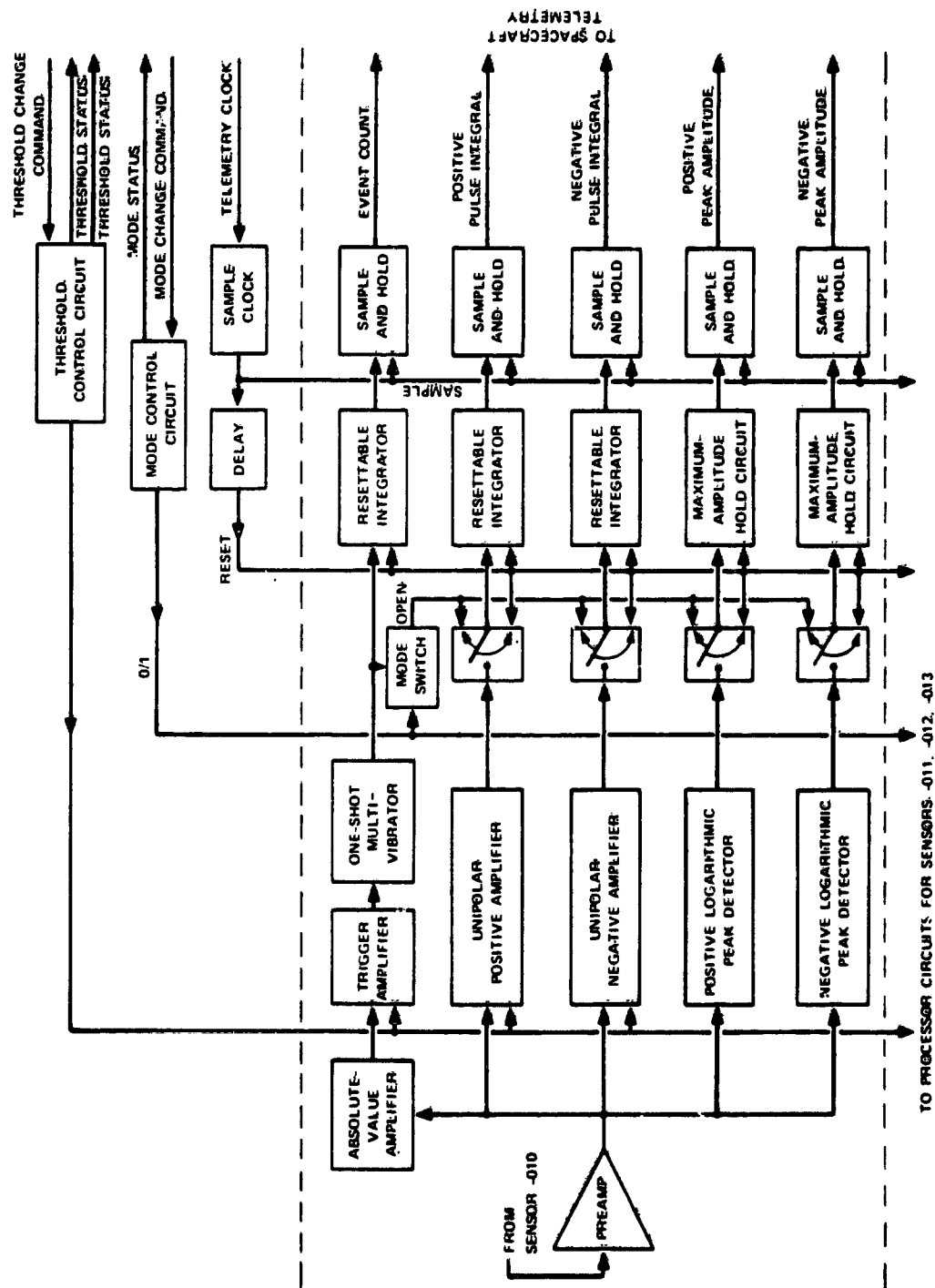
Figure 8. Transient-Pulse Monitor System Functional Block Diagram

733

The sample-and-hold circuit for each output channel is arranged so that data obtained during one telemetry window are transferred to the sample-and-hold where they are stored for one telemetry period during which time all of the output channels are interrogated by the telemetry system. Thus, all of the data read during a particular window were generated during the same single telemetry period.

The pulse-peak detectors indicate the peak amplitude observed during the commanded window. (If several pulses occur, the highest will be measured.) The pulse-integral system indicates the integral over the entire window of that signal above the commanded threshold level. The event-counter indicates the number of pulses occuring during a 1 sec period regardless of which mode is commanded for the pulse-peak and pulse-integral systems.

Packaging of the system is such as to minimize size and weight in order that it can be used as a piggy-back installation with minimum weight, volume, and power impact.

References

1. Nanevicz, J. E., Adamo, R. C., and Scharfman, W. E. (1974) Satellite-Lifetime Monitoring, Final Report Project 2611, Contract FO4701-71-C-0130, Stanford Research Institute, Menlo Park, Calif.

2. Stevens, N. J., Lovell, R. R., and Klinect, V. W. (1976) Preliminary Report on the CTS Transient Event Counter Performance Through the 1976 Spring Eclipse Season, NASA Technical Memorandum NASA TM X-73487, Lewis Research Center, Cleveland, Ohio.